Journal of King Saud University – Science 31 (2019) 1103–1114

Contents lists available at ScienceDirect

Journal of King Saud University – Science

journal homepage: www.sciencedirect.com

Sugarcane juice mediated synthesis of copper oxide nanoparticles, characterization and their antibacterial activity

A.P. Angeline Mary [a], A. Thaminum Ansari [b,*], R. Subramanian [c]

[a] Department of Chemistry, P.S.V. College of Engineering and Technology, Krishnagiri 635108, Tamil Nadu, India
[b] PG & Research Department of Chemistry, Muthurangam Government Arts College (Autonomous), Vellore 632002, Tamil Nadu, India
[c] Department of Chemistry, Sun Arts and Science College, Tiruvannamalai 606755, Tamil Nadu, India

ARTICLE INFO

Article history:
Received 14 July 2018
Accepted 20 March 2019
Available online 21 March 2019

Keywords:
Sugarcane juice
Green synthesis
CuO nanoparticles
Antibacterial activity

ABSTRACT

In this work, an environmental benign, sugarcane juice (SCJ) was applied as an eco-friendly stabilizing agent to synthesize copper oxide nanoparticles (CuO NPs). To produce CuO NPs, 2, 5 and 10 ml of juice were added during the synthesis. The produced CuO NPs were characterized using FTIR, which confirmed the transformation of functional groups through Cu–O. The XRD analysis confirmed the monoclinic crystalline structure and purity of the material. SEM images confirm the nanoparticles formation. Quantitative estimation of Cu, O and C present in samples were carried out by EDS. Square, rectangular, cubic cylindrical and spherical shaped particles observed from the TEM micrographs. Furthermore, Micro-raman and X-ray photoelectron spectroscopy (XPS) were taken to assure the formation of CuO NPs. The results revealed that the SCJ is a good stabilizing agent which reduces the size of particles significantly at higher concentrations and altered shapes to spherical. Hence, it sugarcane juice could be applied as a green stabilizing agent to fabricate the CuO NPs. Antibacterial activity of CuO NPs was assessed against some pathogenic bacteria.

1. Introduction

Research interest in nanoparticles has rapidly improved because of their distinctive physical-chemical properties. Nanomaterials are entirely differing from the bulk materials in terms of diffusivity, electrical resistivity and electrical conducting property. The strength of the nanomaterials and chemical reactivities of nanomaterials differs from the of the bulk materials (Sahooli et al., 2012; Khashan et al., 2016). Metal oxide nanoparticles drawn the attention of researchers due to its wide application in the area of catalysis, sensor and in medical applications. The metal oxide nanoparticles have been proved as disinfectant in the medical field, antimicrobial agent, fillers in cosmetics and as catalysts in industrial field. Metal oxide possessed good semiconducting properties and hence they have been used microelectronics (Katwal et al., 2015). Cupric oxide (CuO) is well known and very smart semiconducting materials which possessed constricted band gap of 1.2 eV (Chen et al., 2013). Outstanding characteristics such as thermal stability, optical properties and electrical conductivity of copper oxide inspired the researcher to work on this material for photocatalytic activity and electrical conductivity (Devi et al., 2014; Bhattacharjee and Ahmaruzzaman, 2016; Eibl, 1993). The application of CuO is mostly acknowledged solar energy harvesting and energy storage batteries (Rakhshani, 1986; Wang, 2009). The CuO NPs also used in antimicrobial devices. There is a relationship between the efficiency and particle size of the CuO. The morphological aspects and structure of the CuO NPs found to be improved by applying various techniques (Ren et al., 2009). To achieve the desired morphology, various synthesis methods have been employed. Some of the common methods are sonochemical, sol-gel method, chemical precipitation, electrochemical, laser ablation and organic modifiers or surfactant mediated synthesis (Safa et al., 2016; Kayani et al., 2015; Ananth et al., 2015).

CuO has drawn the curiosity of researchers due to its biological properties. Antimicrobial and biocidal properties, which led utilize in the biomedical applications (Nations et al., 2015). Electrical conducting, optical and electrical properties of CuO find its applica-

* Corresponding author.
E-mail address: drthaminum@gmail.com (A. Thaminum Ansari).

Peer review under responsibility of King Saud University.

Production and hosting by Elsevier

https://doi.org/10.1016/j.jksus.2019.03.003
1018-3647/

tions as supercapacitors, infrared filters, storage devices and sensors (Devi et al., 2014; Dagher et al., 2014). It is interesting to know that the size of the particles playing key role in the constructing optical, catalytic, electrical and biological properties (Katwal et al., 2015). Apart from the cosmetic and pharmacological applications, CuO NPs also used as paints and coatings (Ruiz et al., 2015).

The optical property is one of the important properties of CuO NPs, which drastically affect the size, morphology and also the temperature (Zhang et al., 2014; Yang et al., 2014). The dimensions of the particles and the morphology are two major feature influencing magnetic properties of CuO NPs (Rao et al., 2009). The electrical conductivity of the nanoparticles influenced by the size of the particles (Azimi et al., 2015). The experimental procedure also controls the properties of nanomaterials. Beyond the known industrial applications, CuO NPs used in anticancer formulations and detection of viruses in the human body as a part of diagnosis of diseases (Ahamed et al., 2014). However, in chemical synthesis, byproducts produced in all the methods. Chemical synthesis of copper oxide nanoparticles might affect and produce toxic to the environment. To avoid the harmfulness posed by chemicals or byproducts, eco-friendly methods gaining the importance to synthesis the nanoparticles. The plant extract acted as reducing as well as a stabilizing agent in the synthesis of metal and metal oxide nanoparticles Besides, green synthesis is a simple, cheap and environmentally friendly (Sharma et al., 2015).

SCJ mediated synthesis $CdFe_2O_4$, silver based chitosan nanocomposite, novel Schiff base caped silver nanocomplexes, SnO_2 quantum dots and Cl@AgCl a solar light active material and proved their dye degradation property against many organic dyes. The synthesized nanomaterials evaluated for their antibacterial activity and degradation of various dyes. They reported that the SCJ act as reducing, capping and stabilizing agent (Patil et al., 2018; Paulkumar et al., 2017; Elemike et al., 2016; Zaman et al., 2015; Kulkarni et al., 2014).

Sugarcane (*Saccharum officinarum*) is a rich source of sugar present in the juice. SCJ contains reducing sugar and non-reducing sugars (glucose & sucrose). It contains chloride, calcium and sodium ion. This juice is also well known for the presence of food supplements such as malic acid, oxalic acid, citric acid D-gluconic acid. Therefore, an attempt was made to use SCJ as stabilizing agent that can be used to produce the nanoparticles by varying the concentration. The aim of the present work was to synthesis CuO NPs using sugarcane juice as a stabilizing agent and capping agents and analyzes their morphology, size and shape including the bactericidal activity.

2. Materials and methods

2.1. Reagents and materials

Fresh sugarcane juice was obtained from the local vendor and centrifuged at 10,000 rpm for 10 min. The clear juice was segregated from the residue and used as stabilizing agent to synthesis the copper oxide nanoparticles. Copper nitrate was purchased from LobaChemie, Mumbai, India.

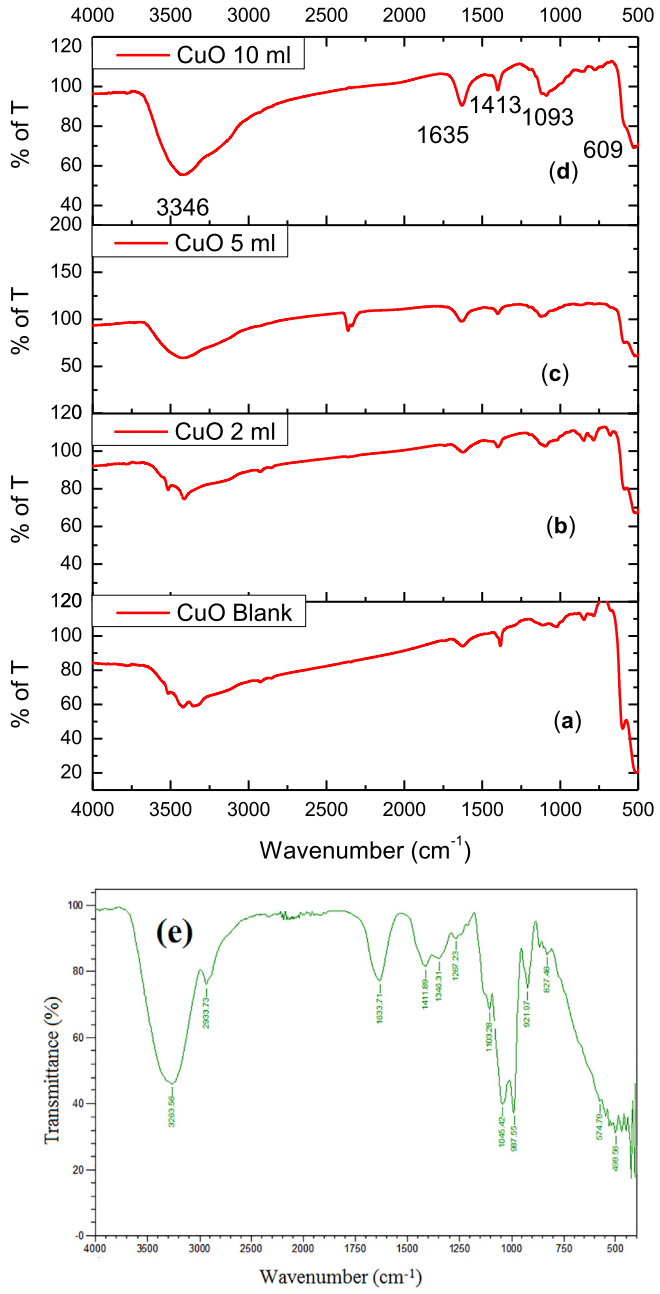

Fig. 1. (a-e). FTIR spectra (a) CuO NPs (b) CuO NPs with 2 ml (c) CuO NPs with 5 ml (d) CuO NPs with 10 ml juice) (e) FTIR spectrum of sugarcane juice.

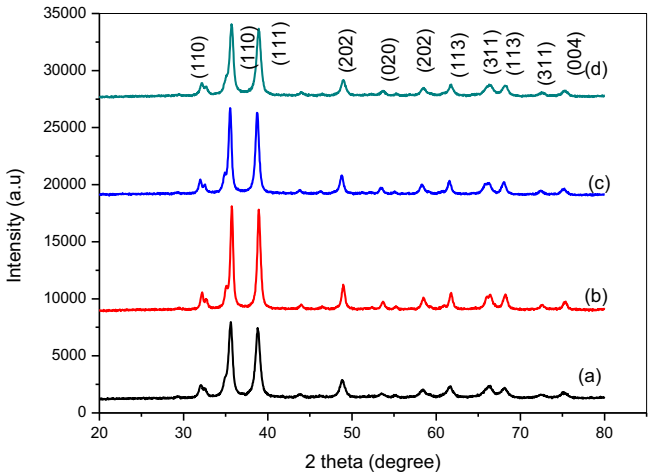

Fig. 2. XRD pattern (a) CuO NPs (b) CuO NPs with 2 ml juice (c) CuO NPs with 5 ml (d) CuO NPs with 10 ml.

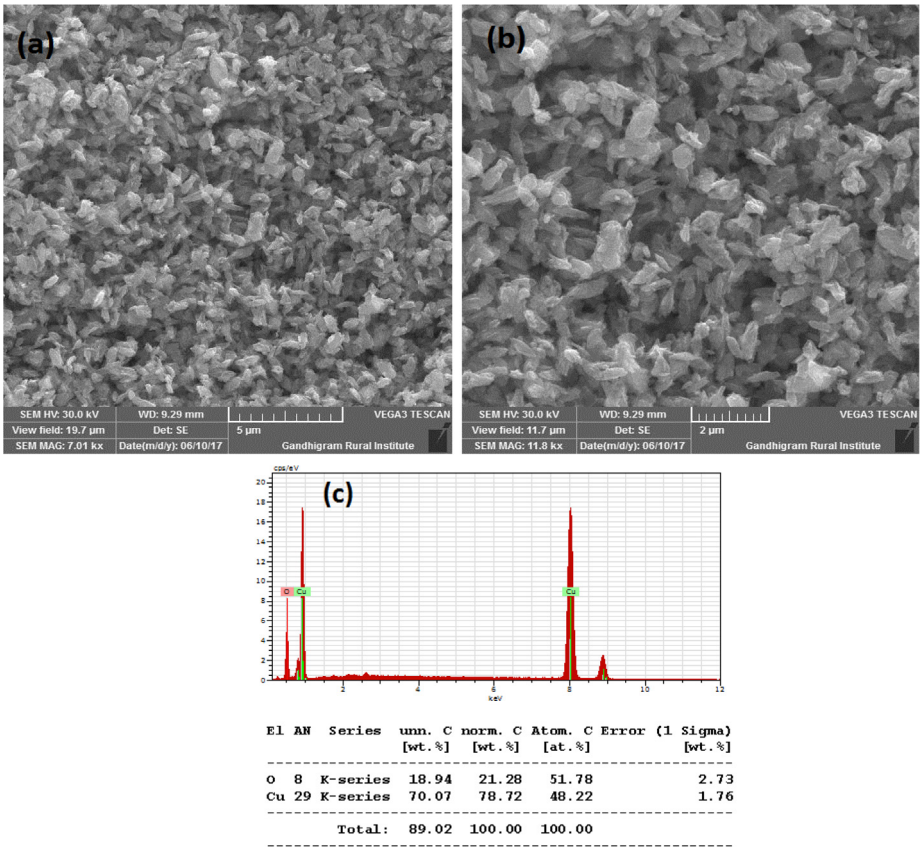

El	AN	Series	unn. C [wt.%]	norm. C [wt.%]	Atom. C [at.%]	Error (1 Sigma) [wt.%]
O	8	K-series	18.94	21.28	51.78	2.73
Cu	29	K-series	70.07	78.72	48.22	1.76
		Total:	89.02	100.00	100.00	

Fig. 3A. (a-c). SEM images and EDS of CuO NPs synthesized without juice.

2.2. CuO NPs synthesis

To synthesize CuO NPs, three different concentrations 2, 5 and 10 ml of juice was mixed with 100 ml of 0.1 M copper nitrate solution and stirred well. Then, the solution was kept on a magnetic stirrer and stirred at 80 °C for an hour. The blue color of reaction mixture turned to green by indicating the development of CuO. Thereafter, an excess amount of 0.5 M ammonium hydroxide was dropwise added to the above solution until the pH reached up to 10 with vigorous stirring. After the addition of ammonium hydroxide, the color of the solution turned to dark brown. The reaction mixture was continued on a magnetic stirrer for 8 h to form the gel. In order to remove the free nitrate ions and organic impurities and excess ammonia, the precipitate obtained was centrifuged and thoroughly washed with distilled water and placed in hot air oven at 80 °C for 8 h. The material was heated at 500 °C for 3 h in a muffle furnace to convert hydroxide into copper oxide.

2.3. Materials characterization

Crystalline property of the CuO NPs was analyzed using advanced diffractometer using Cu–Ka radiation (Model: X'Pert-PRO). Metal-oxygen bond formation was assessed by Fourier transform infrared (Jasco 6300 FT-IR spectrophotometer). The IR spectra of the samples were measured by KBr pellets. Formation of the CuO was identified by scanning electron microscope with the resolution of 15 nm (JEOL Model JSM – 6390LV). The magnification of the instrument was 5×3, 00,000 (both in high and low vacuum modes). The surface morphology of particles was studied using transmission electron microscope (TEM) with resolution (Point: 0.23 nm, Lattice: 0.14 nm) (Jeol/JEM 2100). The percentage copper, oxygen and carbon present in the samples were analyzed by energy dispersive study (EDS). Raman spectra of the nanoparticles was studied by Raman scattering using the 514 nm line with Argon laser source. We also employ microscopic Raman spectroscopy to characterize the cupric particles obtained by X-ray irradiation. Electronic states of CuO NPs were studied using X-ray Photoelectron Spectroscopy (XPS) with Auger Electron Spectroscopy (AES) Module: Model/Supplier: PHI 5000 Versa Prob II, FEI Inc. s.

2.4. Antibacterial activity

Antibacterial activity of CuO NPs was tested using the agar well diffusion method against *Escherichia coli*, *Pseudomonas aeruginosa*, *Staphylooccus aureus* and *Bacillus subtilis* (Elango et al., 2018). Bacterial culture (Mueller Hinton agar) 20 ml was transferred into Petri plates. The wells were punched into the agar plate. The bacteria culture was swabbed on the agar plates. CuO NPs, 100 mg/ml dispersed in DMSO were weighed down into the each well. The petri plates were incubated at 37 °C. The zone of inhibition was noted after 24 h of incubation and expressed in mm dia and compared to the reference substance (Ciprofloxacin). The tests

were performed in triplicates. 25 μg of Ciprofloxacin and 100 μg of CuO NPs were used to test the bactericidal activity.

3. Results and discussion

3.1. FTIR studies

The functional group transformation is identified using the stretching frequencies obtained using FT-IR spectra. Cu–O bond formation, metal-O stretching and presence of hydroxyl, and moisture content were characterized using FT-IR spectral techniques. The FT-IR spectra of CuO NPs produced by green route are presented in Fig. 1(a-d). A peak observed at 609 cm^{-1} due to stretching vibrations of Cu–O bond in CuO NPs. Two peaks shown at 799 and 855 cm^{-1} are revealed the M−O stretching vibrations of CuO NPs (Thekkae Padil et al., 2013; Xu et al., 2007). The absorption peaks observed at 1635 and 3346 cm^{-1} contribute to the bending and stretching vibrations of moisture content present on the surface of CuO NPs. The peaks noticed near 500–600 cm^{-1} indicate the metal–oxygen vibration frequencies of copper and oxygen (Kuppusamy et al., 2017; Taghavi Fardood et al., 2016). Components of sugarcane juice are high molecular weight polysaccharide and protein moieties. To assure this study, the FTIR examination of the sugarcane juice was performed (Fig. 1e). There are three characteristic peaks at wave numbers 827–1045, 1517 and 1631 cm^{-1} present in both the samples analyzed. In general, the peak intensities for the polysaccharide fraction are higher except at 1517 and 1631 cm^{-1}. It showed peaks at 3263 (high molecular weight), 2933, 1633, 1048, 1411, 1346 and 1267 cm^{-1} corresponds to OH, C–H stretching, C═O, O–C═O, C–H stretching of the aromatic ring, phenolic OH and C–C stretching of various molecules. Small peaks noticed at 103 and 887–827 cm^{-1} attributed to β-glycosidic linkage between sugars. The observed peaks correspond to characteristic protein and polysaccharide bands (Guilherme et al., 2015; Camargo et al., 2012).

3.2. XRD analysis

The XRD system was utilized to establish and authenticate the crystalline nature of the CuO NPs. The XRD spectra of the CuO NPs are shown in Fig. 2(a-d). The XRD report revealed a sequence of diffraction peaks at 2θ of X-axis at 32.11°, 35.62°, 38.87°, 48.85°, 53.49°, 58.46°, 61.71° and 66.5° matching for the (1 1 0), (1 1 1), (2 0 0), (−2 0 2), (0 2 0), (2 0 2), (−1 1 3) and (0 2 2) planes, correspondingly. The XRD spectrum evidently suggested the crystalline nature and purity of the CuO. All the diffraction peaks are identical to the mono-clinic phase structure. Further, it was cross checked with existing JCPDS data (80–1916) (Kuppusamy et al., 2017). No impurities other than CuO NPs were noticed in the

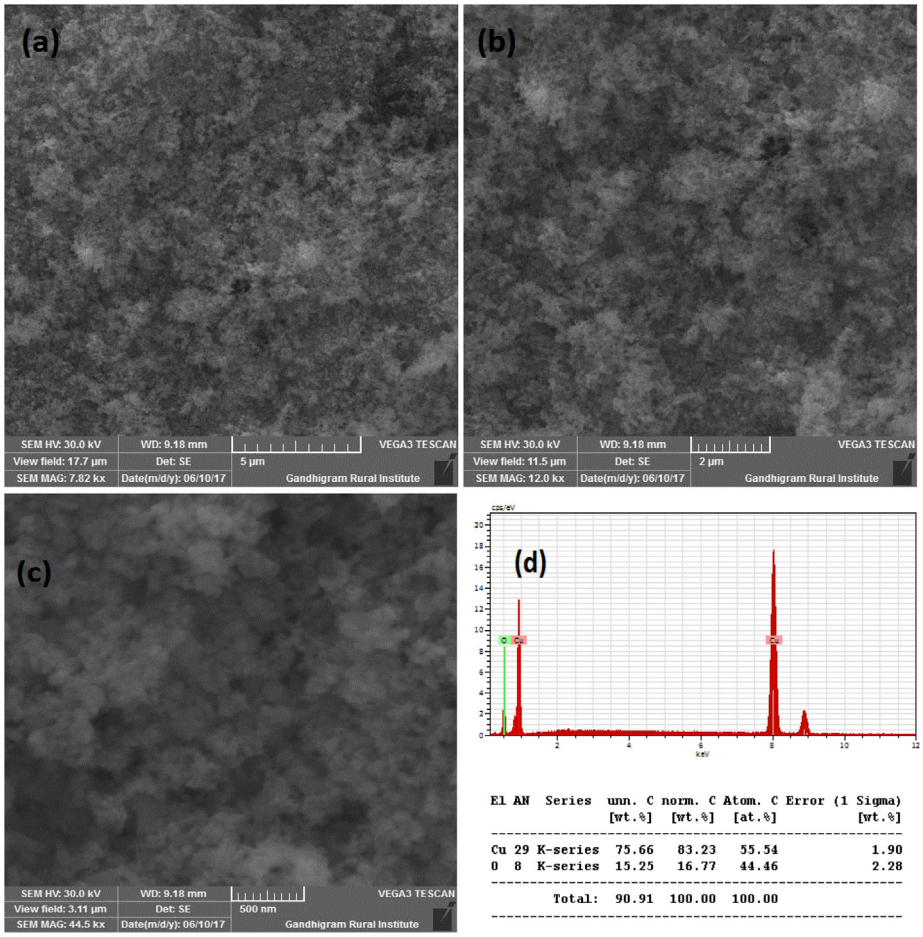

Fig. 3B. (a-d). SEM images and EDS of CuO NPs with 2 ml juice.

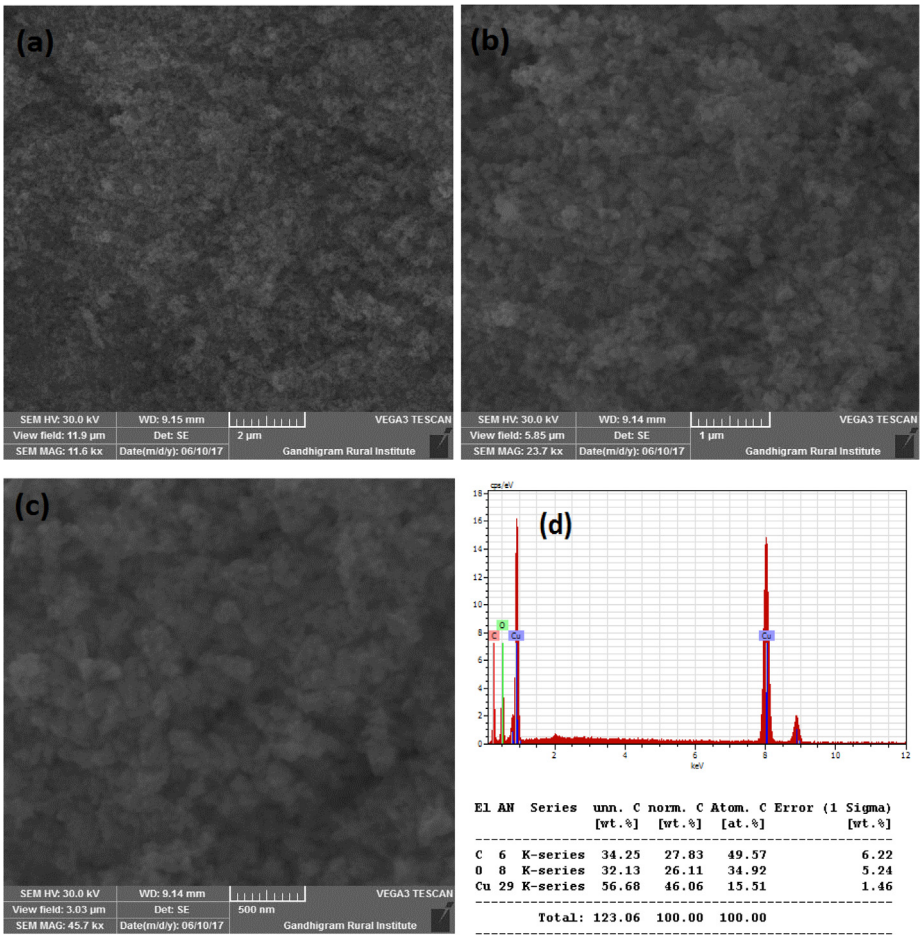

Fig. 3C. (a-d). SEM images and EDS of CuO NPs synthesized with 5 ml juice.

XRD peaks representing the high phase purity. The average crystallite size of CuO NPs synthesized using 2, 5 and 10 ml juice and blank CuO were found to be 29.89, 23.61, 23.93 and 22.80 nm.

3.3. SEM and EDS study

Fig. 3A(a-b) show the SEM images of CuO synthesized without SCJ. As seen in the figure, SEM images showed lengthy particles with irregular shapes. The quantity of Cu and O confirmed by energy dispersive (EDS) study as shown in Fig. 3A(c). The SEM images and elemental analysis of Cu NPs synthesized using 2, 5 and 10 ml juice is shown in Fig. 3B(a-c), Fig. 3C(a-c) and Fig. 3D(-a-c). The SEM images exhibited agglomerated particles as seen in the figure. Though the specific shapes were not observed from the SEM images, but it confirmed the formation of nanoparticles. The morphology of CuO NPs synthesized using 2 and 5 ml juice appeared to be similar in morphology. However, CuO NPs synthesized using 10 ml juice found to be spherical in shape. The EDS analysis revealed the percentage of Cu and O present in the samples. The Cu and O existed in the blank CuO found to be 75.66 and 15.25% (Fig. 3A(c). The CuO with 2 ml showed 55.54% of Cu and 44.46% of O (Fig. 3B(c). The percentage of C content was not observed in this sample. The elemental composition of CuO NPs synthesized using 5 and 10 ml showed C in addition to Cu and O. The percentage of Cu, O and C present in CuO with 5 ml juice found to be 56.60, 32.13 and 34.25% (Fig. 3C(c). The CuO NPs produced with 10 ml juice showed 63.91, 22.11 and 7.99% of Cu, O and C atoms (Fig. 3D(c). The C content must be derived from the sucrose present in the juice. The significant decrease in C content in CuO NPs synthesized using 10 ml juice is unclear. Because, all the samples were heat treated at 500 °C for 3 h.

3.4. TEM analysis

As shown in Fig. 4A(a-d), TEM micrographs of CuO NPs synthesized without juice exhibited agglomerated particles. The average size of the particles calculated was 84.40 nm. It exhibited irregular shapes as seen in the images. The CuO NPs produced with 2 ml juice showed well separated particles. It exhibited spherical, square, cube, plate, rectangular with some irregular shapes when 5 ml of juice was used (Fig. 4B(a-f)). For 5 ml, nanoparticles showed similar shapes as shown by 2 ml juice (Fig. 4C(a-d)). The average size of the particles synthesized using 2, 5 and 10 ml of juice measured from the TEM images were 60.50, 40.40 and 29.50) nm, respectively. The gradual addition of the juice (2, 5 and 10 ml) rapidly reduced the size of the particles (60.50, 40.40 and 29.50 nm). The existence of inter-planar spacing of 0.23 nm of CuO with 2 and 5 ml representing the perfect orientation (2 0 0) of the nanoparticles. CuO NPs produced by 10 ml juice showed spherical shaped particles might be due to the attractive force between the molecules and the CuO NPs (Fig. 4D(a-f). It is well known that sugarcane juice contains glucose and fructose as

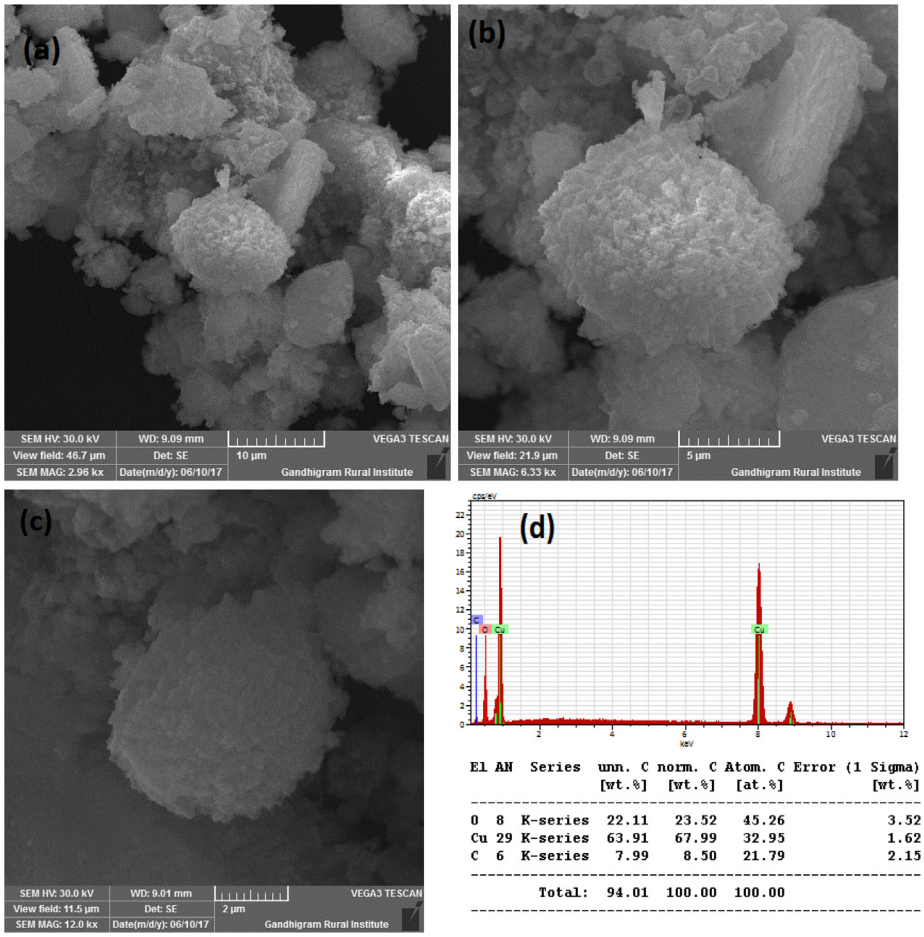

Fig. 3D. (a-d). SEM images and EDS of CuO NPs with 10 ml juice.

major components and other organic acids as minor components. It has been proved that the sugar molecule and organic acids can act as a surface modifier, stabilizing and capping agents, which proved to control the size, shape and morphology (Sharma et al., 2015; Bhattacharjee and Ahmaruzzaman, 2016). The formation of CuO nanoparticles is proposed by the following mechanism as given in equations (1) and (2). Copper nitrate is reduced into copper hydroxide when ammonium hydroxide was added. In the presence of sugarcane juice, copper hydroxide was calcinated at 400 °C to form copper oxide. We believed that the interaction between glucose and fructose present in the sugarcane juice and copper hydroxide led to the formation of various shapes of particles. As the volume of juice increases, spherical shaped particles appeared predominantly as shown in (Fig. 4D(a-f). Stability of the colloids was monitored in the laboratory. After three months, particles settled down completely.

$$Cu(NO_3)_2 + 2(NH_3.2H_2O) \rightarrow Cu(OH)_2 + 2NH_4NO_3 \quad (1)$$

$$Cu(OH)_2 + C_{12}H_{22}O_{11}(\text{Sucrose}) \xrightarrow{400 \text{ degree C}} CuO + H_2O \quad (2)$$

3.5. Raman spectra

Raman spectroscopy is a main tool to identify the local atomic arrangements and vibrations of the metal oxides, which helps to analyze the structural nature of the micro and nanoparticles. Raman spectra of plain CuO NPs and one CuO NPs synthesized using 10 ml of sugarcane juice are representative samples are shown Fig. 5(a,b). Raman spectra of pure CuO NPs showed peaks at 280, 332 and 616 cm^{-1}. Sugarcane juice stabilized CuO NPs showed peaks at 285, 335 and 620 cm^{-1}. The peak assignment at 280–285 cm^{-1} to the Ag mode of vibration, while the other two peaks at 332–335 and 616–620 cm^{-1} assigned to the Bg modes (Irwin et al., 1990). The oxygen atoms only shift with a dislocation in the b-direction for Ag and perpendicular to the b-axis for Bg Raman modes (Gan et al., 2004). It was proven that the Raman shift and bandwidth alter with decreasing the size of the particles (Swarnkar et al., 2011; Rashad et al., 2013).

3.6. XPS analysis

The survey scan of XPS for pure CuO and CuO NP synthesized using sugarcane juice is presented Fig. 6(a). The elements such as Cu, C, and O are all indexed. The peaks corresponding to Cu 3d, 3p, 3s, 2p and Auger, O 1s are apparently noticed. C 1s peak is also noticed. Peak for argon is not found, revealing that no argon present in the samples. The XPS spectra consequent to Cu 2p and O 1s are shown in Fig. 6 (a-d). The binding energy of 283.47 eV reveals the C 1s peak. The relevant major peaks

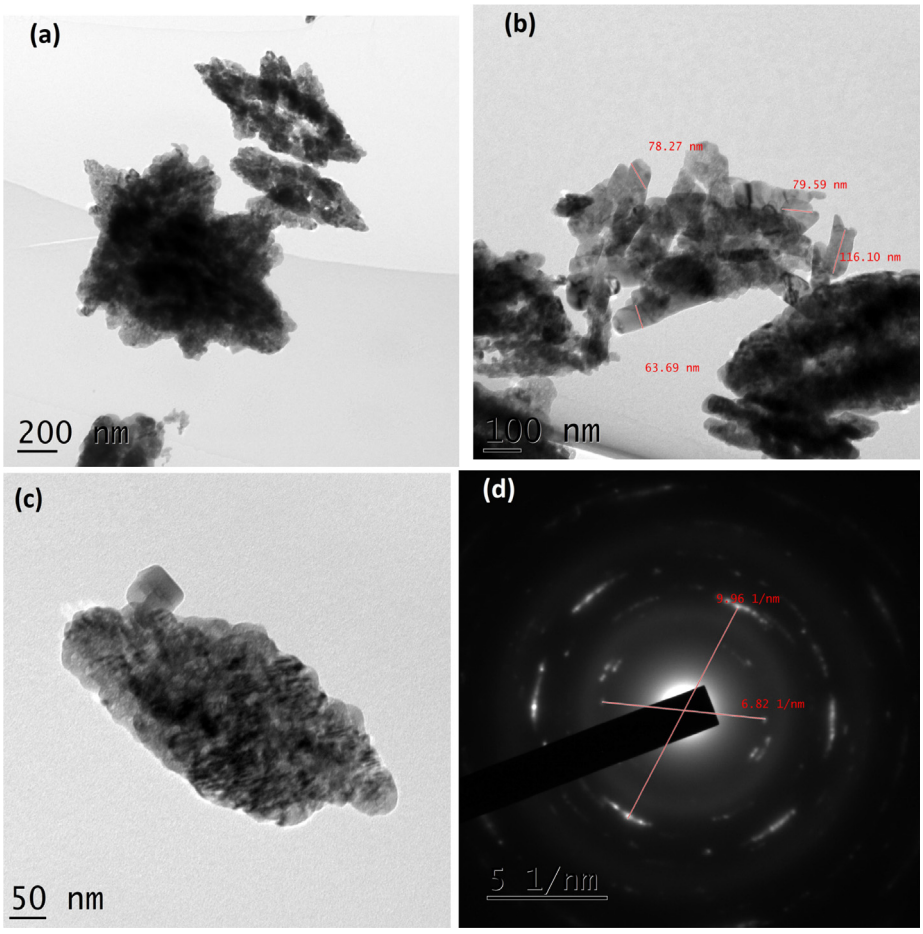

Fig. 4A. (a-d). TEM images and SAED pattern of CuO NPs.

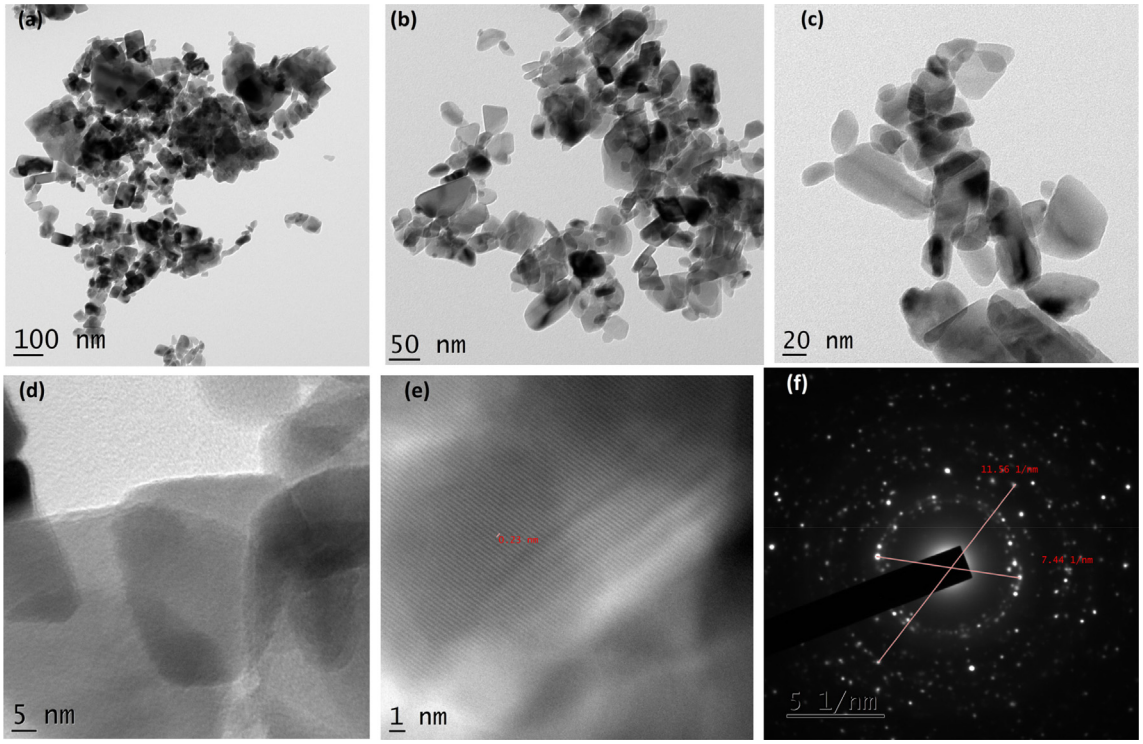

Fig. 4B. (a-f). TEM images and SAED pattern of CuO with 2 ml juice.

of Cu $2p_{3/2}$ for pure CuO and CuO NPs synthesized using 2, 5 and 10 ml of juice lie at 932.17 and 941.63 eV. Fig. 6 (a-d) with well-built fitting 952.98 and 961.58 eV for Cu $2p_{1/2}$ (Gao et al., 2010). The calculated gap between the Cu $2p_{3/2}$ and Cu $2p_{1/2}$ is 19.95 eV, which is in concurrence with the normal value of 20.0 eV for CuO (Lin et al.,2004). This gives strong evidence of an $3d^9$ shell resultant to the Cu^+ state. Further, Fig. 6 (a-d) shows the XPS spectra of O 1 s. Also, a peak observed at lower binding energy region is assigned to O^{2-} of CuO nanoparticles. A major peak at the lower peak at 529.4 eV is ascribed to Cu–O (Nagajyothi et al., 2017).

3.7. Bactericidal activity

25 μg of Ciprofloxacin and 100 μg of CuO NPs were used to test the bactericidal activity.

The zone of inhibition shown by CuO NPs synthesized using 10 ml juice against *Escherichia coli*, *Pseudomonas aeruginosa*, *Staphylooccus aureus* and *bacillus subtilis* was 5, 8 and 9 mm (Fig. 7(-A-D)). All bacteria showed more or less inhibition, especially 10 ml juice. Whereas, 2 and 5 ml juice stabilized CuO NPs showed 5, 7 and 9 mm zone of inhibition. The zone of inhibition of shown by the NPs is comparable (12 mm) with reference compound (Ciprofloxacin).

Various mechanisms have been widely proposed by the researcher for the antibacterial activity of the nanoparticles. Penetration of smallest particles into the cell walls of the bacteria and binding of nanoparticles with the nucleic acids of bacteria also causes severe toxic (Elango et al., 2017). It is well known sugarcane juice contains monosaccharides (glucose and fructose), doscaccharides (sucrose), minerals and amino acids. According to literature, sugarcane juice contains 81–87% and 3–6% of reducing sugars and remaining constituents includes minerals and amino acids (Walfors, 1996). The presence of sugar moieties was confirmed by FT-IR spectrum of sugarcane juice. Various plant extracts mediated green synthesis of CuO NPs and their size including morphology from the literature is presented in Table 1. The green synthesis of CuO NPs using aqueous extract of various parts of plant extract revealed the spherical shaped particles. Range of size starting from 5 nm to 140 nm of CuO NPs fornd in literature (Table 1). We obtained spherical shaped CuO NPs at higher concentration. At lower concentration, in addition to spherical, various shapes such as square, cube, plate, rectangular with some irregular shapes obtained. The size and shapes of the

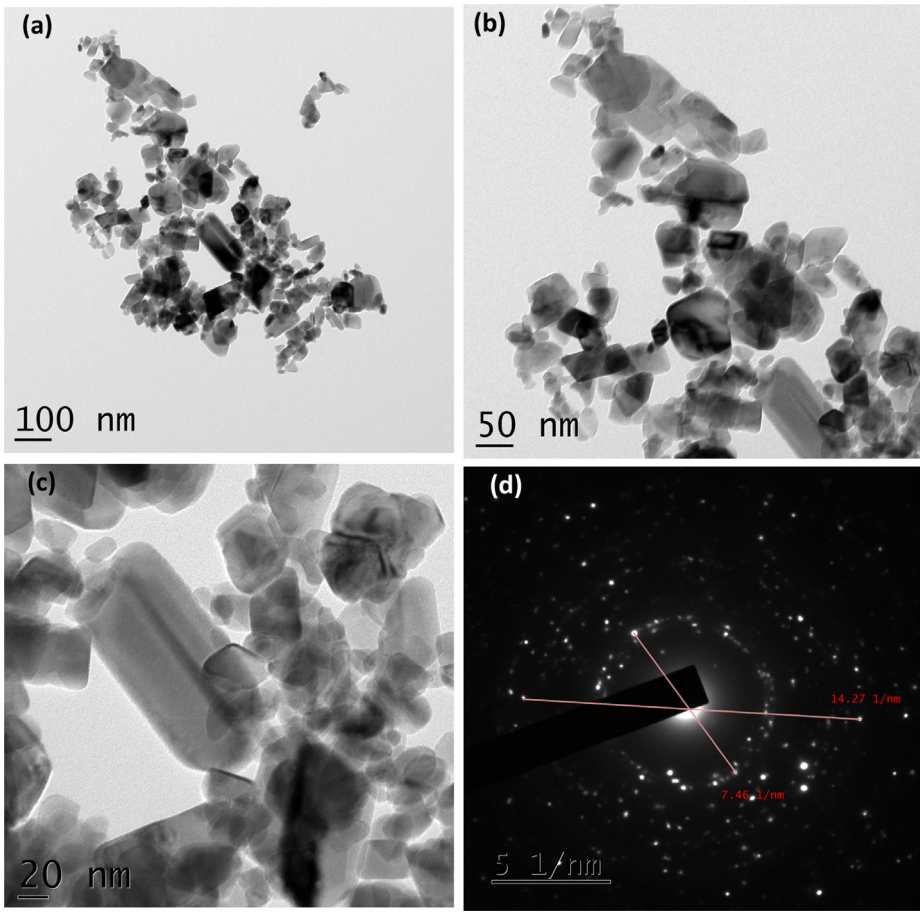

Fig. 4C. (a-d). TEM images and SAED pattern of CuO with 5 ml juice.

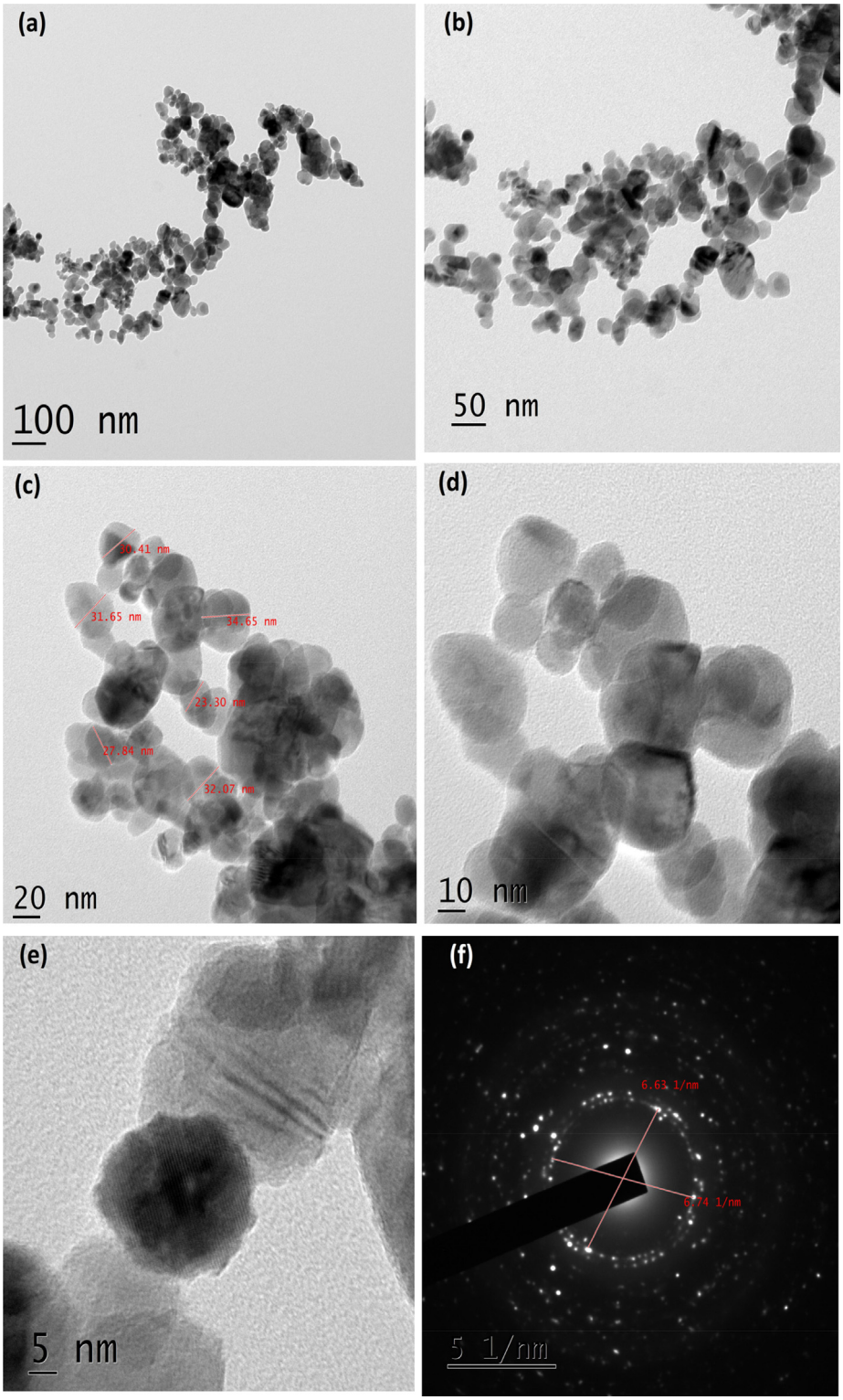

Fig. 4D. (a-f). TEM images and SEAD pattern of CuO NPs with 10 ml juice.

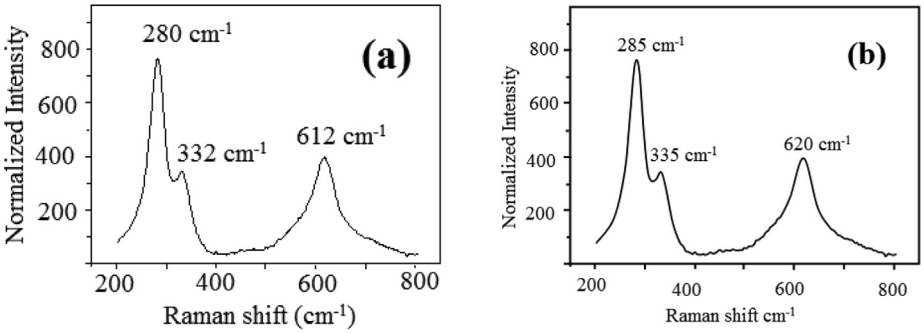

Fig. 5. (a, b). Raman spectra (a) Pure CuO (b) CuO NPs with 10 ml juice.

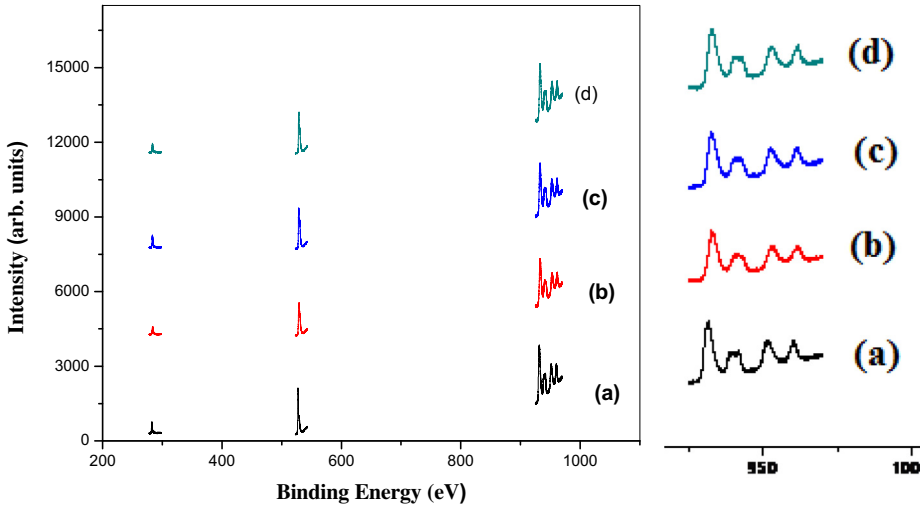

Fig. 6. (a-d). XPS spectr (a) Pure CuO, (b) CuO with 2 ml, (c) CuO with 5 ml, (d) CuO with 10 ml juice.

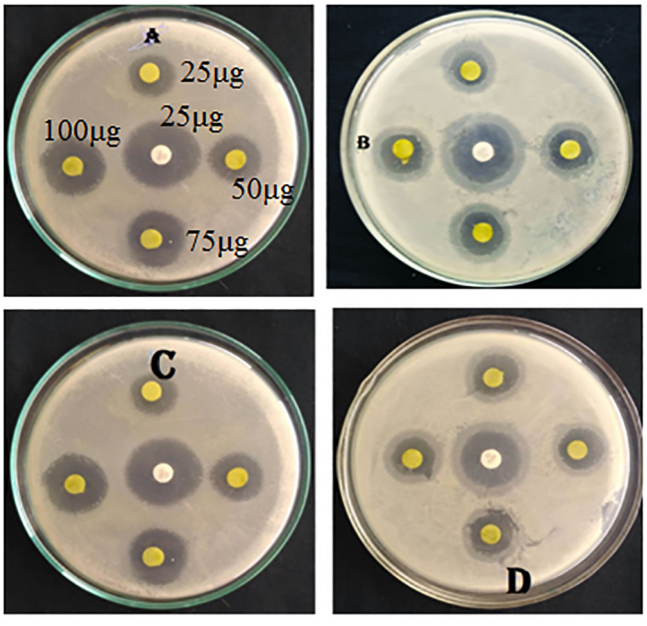

Fig. 7. (A-D). Antibacterial activity of CuO NPs: Zone of inhibition of (A) *Escherichia coli* (B) *Pseudomonas aeruginosa* (C) *Staphylooccus aureus* and (D) *bacillus subtilis*.

CuO NPs synthesized using sugarcane was comparable with literature.

4. Conclusions

The present study report the eco-friendly and convenient greener route synthesis of CuO nanoparticles using SCJ as a stabilizing agent. FTIR and XRD pattern of the samples proved the formation of CuO NPs and their crystalline structure. The SEM images confirmed formation of particles in nanoscale. The TEM images confirmed the existence spherical, square, cubic and rectangular shaped nanoparticles at lower concentrations. Sugarcane juice rapidly reduced the size of the particles in higher concentration. In addition, the above mentioned various shapes of particles disappeared at higher concentrations and produced spherical shaped particles. This work proved that the sugarcane is a suitable green stabilizing agent to produce copper oxide nanoparticles. Further, formation CuO NPs supported by the Raman spectra and XPS analysis. Synthesized CuO NPs exhibited significant bactericidal activity against *Escherichia coli, Streptococcus aureus, Pseudomonas aeruginosa* and *bacillus subtilis*. Synthesis of well dispersed copper oxide nanoparticles suggesting that the sugarcane juice acting as a capping well as stabilizing agent and put off the agglomeration, and provides stability to medium

Table 1
Green synthesis of CuO NPs and their size, shape and morphology.

S. No	Name of the plant	Size of the Particle (nm)	Shape and Morphology	References
1.	Caloropis procera	46	cylindrical	Rayapa Reddy, 2017
2.	Oak Fruit Hull	34	quasi-spherical	Sorbiun et al., 2018
3.	Syzygium alternifolium	13–17	spherical	Yugandhar et al., 2017
4.	Gloriosa superba L	5–10	spherical	Raja Naika et al., 2015
5.	Solanum tuberosum	54	spherical	Alishah et al., 2016
6.	Banana peel	60	Spherical	Aminuzzaman et al., 2017
7.	Dry black beans	26	Spherical	Nagajyothi et al., 2017
8.	Aloe vera leaf	20	Spherical	Vijay Kumar et al., 2015
9.	Bauhinia tomentosa	22–40	Spherical	Sharmila et al., 2018
10.	Azadirachta indica	48	Cubical	Nagar and Devra, 2018
11.	Punica granatum	40	Spherical	Ghidan et al., 2016
12.	Rheum palmatum L	30	Spherical	Bordbar et al., 2016
13.	Chamomile flower	140	Sphere	Fatih Duman et al., 2016

Conflict of interest

No conflict of interest declared by the authors regarding this manuscript.

References

Aminuzzaman, M., Mei Kei, L., Hong Liang, W., 2017. Green synthesis of copper oxide (CuO) nanoparticles using banana peel extract and their photocatalytic activities. AIP Conference Proceedings 1828, 020016.

Ananth, A., Dharaneedharan, S., Heo, M.-S., Mok, Y.S., 2015. Copper oxide nanomaterials: synthesis, characterization and structure-specific antibacterial performance. Chem. Eng. J. 262, 179–188.

Azimi, H., Taheri, R., 2015. Electrical conductivity of CuO nanofluids. Int. J. Nano Dimens. 6, 77.

Ahamed, M., Alhadlaq, H.A., Khan, M., Karuppiah, P., Al-Dhabi, N.A., 2014. Synthesis, characterization, and antimicrobial activity of copper oxide nanoparticles. J. Nanomater. 5, 519–524.

Alishah, H., Pourseyedi, S., Yousef Ebrahimipour, S., Esmaili Mahani, S., Rafiei, N., 2017. Green synthesis of starch-mediated CuO nanoparticles: preparation, characterization, antimicrobial activities and in vitro MTT assay against MCF-7 cell line. Rend. Fis. Acc. Lincei 28, 65–71.

Bhattacharjee, A., Ahmaruzzaman, M., 2016. CuO nanostructures: facile synthesis and applications for enhanced photodegradation of organic compounds and reduction of pnitrophenol from aqueous phase. RSC Adv. 6, 41348–41363.

Camargo, F.A., Innocentini-Mei, L.H., Lemes, A.P., Moraes, S.G., Duran, N., 2012. Processing and characterization of composites of poly (3-hydroxybutyrateco-hydroxyvalerate) and lignin from sugar cane bagasse. J. Compos. Mater. 46, 417–425.

Chen, H., Zhao, G., Liu, Y., 2013. Low-temperature solution synthesis of CuO nanorods with thin diameter. Mater. Lett. 93, 60–63.

Devi, H.S., Singh, T.D., 2014. Synthesis of copper oxide nanoparticles by a novel method and its application in the degradation of methyl orange. Adv. Electr. Electron. Eng. 4, 83–88.

Dagher, S., Haik, Y., Ayesh, A.I., Tit, N., 2014. Synthesis and optical properties of colloidal CuO nanoparticles. J. Lumin. 151 (2014), 149–154.

Duman, F., Ocsoy, I., Ozturk Kup, F., 2016. Chamomile flower extract-directed CuO nanoparticle formation for its antioxidant and DNA cleavage properties. Mater. Sci. Eng. C 60, 333–338.

Elango, M., Deepa, M., Subramanian, R., Saraswathy, G., 2018. Synthesis, structural characterization and antimicrobial activities of polyindole stabilized Ag-Co_3O_4 nanocomposite by the reflux condensation method. Mater. Chem Phys. 216, 305–315.

Elango, M., Deepa, M., Subramanian, R., Mohamed Musthafa, A., 2017. Synthesis, characterization of polyindole/Ag-ZnO nanocomposites and its antibacterial activity. J. Alloys Compds. 696, 391–401.

Elemike, E.E., Darebc, E.O., Samuel, I.D., Onwuk, J.C., 2016. 2-Imino-(3,4-dimethoxybenzyl) ethanesulfonic acid Schiff base anchored silver nanocomplex mediated by sugarcane juice and their antibacterial activities. J. Appl. Res. Technol. 14, 38–46.

Eibl, O., 1993. Application of a new method for absorption correction in high-accuracy, quantitative EDX microanalysis in the TEM: analysis of oxygen in CuO-based high-Tc superconductors. Ultramicroscopy 50, 189–201.

Guilherme, A., Dantas, P.V.F., Santos, E.S., Fernandes, F.A.N., Macedo, G.R., 2015. Evaluation of composition, characterization and enzymatic hydrolysis of pretreated sugar cane bagasse. Brazilian J. Chem. Eng. 32, 23–33.

Gan, Z.H., Yu, G.Q., Tay, B.K., Tan, C.M., Zhao, Z.W., Fu, Y.Q., 2004. Preparation and characterization of copper oxide thin films deposited by filtered cathodic vacuum arc. J. Phys. D: Appl. Phys. 37 (2004), 81–85.

Gao, D., Zhang, J., Zhu, J., Qi, J., Zhang, Z., Sui, W., Shi, H., Xue, D., 2010. Vacancy-mediated magnetism in pure copper oxide nanoparticles. Nanoscale Res. Lett. 5, 769–772.

Ghidan, A.Y., Al-Antary, T.M., Awwad, A.M., 2016. Green synthesis of copper oxide nanoparticles using *Punica granatum* peels extract: effect on green peach Aphid. Environ. Nanotechnol. Monit. Manage. 6, 95–98.

Irwin, J.C., Chrzanowski, J., Wei, T., Lockwood, D.J., Xin, X.Q., 1990. Raman scattering from single crystals of cupric oxide. Phys. C 166, 456–464.

Kuppusamy, P., Ilavenil, S., Srigopalram, S., Maniam, G.P., Yusoff, M.M., Govindan, N., 2017. Treating of palm oil mill effluent using *Commelina nudiflora* mediated copper nanoparticles as a novel biocontrol agent. J. Clean. Prod. 141, 1023–1029.

Khashan, K.S., Sulaiman, G.M., Abdulameer, F.A., 2016. Synthesis and antibacterial activity of CuO nanoparticles suspension induced by laser ablation in liquid. Arab. J. Sci. Eng. 41, 301–310.

Katwal, R., Kaur, H., Sharma, G., Naushad, M., Pathania, D., 2015. Electrochemical synthesized copper oxide nanoparticles for enhanced photocatalytic and antimicrobial activity. J. Ind. Eng. Chem. 31, 173–184.

Kayani, Z.N., Umer, M., Riaz, S., Naseem, S., 2015. Characterization of copper oxide nanoparticles fabricated by the sol-gel method. J. Electron. Mater. 44, 3704–3709.

Kulkarni, A.A., Bhanage, B.M., 2014. Ag@AgCl nanomaterial synthesis using sugarcane juice and its application in degradation of azo dyes. ACS Sustain. Chem. Eng. 2, 1007–1013.

Lin, H.H., Wang, C.Y., Shih, H.C., Chen, J.M., Hsieh, C.T., 2004. Characterizing well-ordered CuO nanofibrils synthesized through gas-solid reactions. J. Appl. Phys. 95, 5889–5895.

Nations, S., Long, M., Wages, M., Maul, J.D., Theodorakis, C.W., Cobb, G.P., 2015. Subchronic and chronic developmental effects of copper oxide (CuO) nanoparticles on *Xenopus laevis*. Chemosphere 135, 166–174.

Nagajyothi, P.C., Muthuraman, P., Sreekanth, T.V.M., Kim, D.H., Shim, J., 2017. Green synthesis: in-vitro anticancer activity of copper oxide nanoparticles against human cervical carcinoma cells. Arab. J. Chem. 10, 215–225.

Nagar, N., Devra, V., 2018. Green synthesis and characterization of copper nanoparticles using *Azadirachta indica* leaves. Mater. Chem. Phys. 213, 44–51.

Patil, S.B., Bhojya Naik, H.S., Nagaraju, G., Shiralgi, Y., 2018. Sugarcane juice facilitated eco-friendly synthesis of solar light active $CdFe_2O_4$ nanoparticles and its photocatalytic application. Eur. Phys. J. Plus 133, 229.

Paulkumar, K., Gnanajobitha, G., Vanaja, M., Pavunraj, M., Annadurai, G., 2017. Silver based citosan bionanocomposite using stem extract of *Saccharum officinarum* and assessment of its antibacterial activity. Adv. Nat. Sci. Nanosci. Nanotechnol. 8, 035019.

Ruiz, P., Katsumiti, A., Nieto, J.A., Bori, J., Jimeno-Romero, A., Reip, P., Arostegui, I., Orbea, A., Cajaraville, M.P., 2015. Short-term effects on antioxidant enzymes and long-term genotoxic and carcinogenic potential of CuO nanoparticles compared to bulk CuO and ionic copper in mussels *Mytilus galloprovincialis*. Mar. Environ. Res. 111, 107–120.

Rao, G.N., Yao, Y., Chen, J., 2009. Evolution of size, morphology, and magnetic properties of CuO nanoparticless by thermal annealing. J. Appl. Phys. 105, 093901.

Rayapa Reddy, K., 2017. Green synthesis, morphological and optical studies of CuO nanoparticles. J. Mol. Struct. 1150, 553–557.

Rakhshani, A.E., 1986. Preparation, characteristics and photovoltaic properties of cuprous oxide-a review. Solid State Electron. 29, 7–17.

Rashad, M., Rüsing, M., Berth, G., Lischka, K., Pawlis, A., 2013. CuO and Co_3O_4 nanoparticles: synthesis, characterizations, and Raman spectroscopy. J. Nanomater. 2013. Article ID 714853, 6.

Raja Naika, H., Lingaraju, K., Manjunath, K., Kumar, Danith, Nagaraju, G., Suresh, D., Nagabhushana, H., 2015. Green synthesis of CuO nanoparticles using *Gloriosa superba* L. extract and their antibacterial activity. J. Taibah Univ. Sci. 9, 7–12.

Ren, G., Hu, D., Cheng, E.W.C., Vargas-Reus, M.A., Reip, P., Allaker, R.P., 2009. Characterisation of copper oxide nanoparticles for antimicrobial applications. Int. J. Antimicrob. Agents 33, 587–590.

Safa, S., Azimirad, R., Moghaddam, S.S., Rabbani, M., 2016. Investigating on photocatalytic performance of CuO micro and nanostructures prepared by different precursors. Desalin. Water Treatment 57 (2016), 6723–6731.

Sharma, J.K., Akhtar, M.S., Ameen, S., Srivastava, P., Singh, G., 2015. Green synthesis of CuO nanoparticles with leaf extract of *Calotropis gigantea* and its dye-sensitized solar cells applications. J. Alloys Compds. 632, 321–325.

Sharmila, G., Sakthi Pradeep, R., Sandiya, K., Santhiya, S., Muthukumaran, C., Jeyanthi, J., Manoj Kumar, N., Thirumarimurugan, M., 2018. Biogenic synthesis of CuO nanoparticles using *Bauhinia tomentosa* leaves extract: characterization and its antibacterial application. J. Mol. Struct. 1165, 288–292.

Sahooli, M., Sabbaghi, S., Saboori, R., 2012. Synthesis and characterization of mono sized CuO nanoparticles. Mater. Lett. 81, 169–172.

Swarnkar, R.K., Singh, S.C., Gopal, R., 2011. Effect of aging on copper nanoparticles synthesized by pulsed laser ablation in water: structural and optical characterizations. Bull. Mater. Sci. 34, 1363–1369.

Sorbiun, M., Shayegan Mehr, E., Ramazani, A., Taghavi Fardood, S., 2018. Green synthesis of zinc oxide and copper oxide nanoparticles using aqueous extract of oak fruit hull (Jaft) and comparing their photocatalytic degradation of basic violet 3. Int. J. Environ. Res. 12, 29–37.

Taghavi Fardood, S., Ramazani, A., 2016. Green synthesis and characterization of copper oxide nanoparticles using coffee powder. J. Nanostruct. 6, 167–171.

Thekkae Padil, V.V., Černík, M., 2013. Green synthesis of copper oxide nanoparticles using gum karaya as a biotemplate and their antibacterial application. Int. J. Nanomed. 8, 889–898.

Vijay Kumar, P.P.N., Pratap Kollu, U.S., Kalyani, R.L., Pammi, S.V.N., 2015. Green synthesis of copper oxide nanoparticles using *Aloevera* leaf extract and its antibacterial activity against fish bacterial pathogens. BioNanoSci. 5, 135–139.

Walfors, S.N., 1996. Composition of cane juice. Proc.S. Afr. Sug. Technol. Ass, 70.

Xu, Y., Chen, D., Jiao, X., Xue, K., 2007. CuO microflowers composed of nanosheets: synthesis, characterization, and formation mechanism. Mater. Res. Bull. 42, 1723–1731.

Yang, C., Xiao, F., Wang, J., Su, X., 2014. Synthesis and microwave modification of CuO nanoparticles: crystallinity and morphological variations, catalysis, and gas sensing. J. Colloid Interface Sci. 435 (435), 34–42.

Yugandhar, P., Vasavi, T., Uma Maheswari Devi, P., Savithramma, N., 2017. Bioinspired green synthesis of copper oxide nanoparticles from *Syzygium alternifolium* (Wt.) Walp: characterization and evaluation of its synergistic antimicrobial and activity. Appl. Nanosci. 7, 417–427.

Wang, H., Pan, Q., Zhao, J., Chen, W., 2009. Fabrication of CuO/C films with sisal-like hierarchical microstructures and its application in lithium ion batteries. J. Alloys Compds. 476, 408–413.

Zaman, M.A., Bhattacharjee, A., 2015. Photocatalytic-degradation and reduction of organic compounds using SnO_2 quantum dots (via green route) under direct sunlight. RSC Adv. 5, 66122–66133.

Zhang, Q., Zhang, K., Xu, D., Yang, G., Huang, H., Nie, F., Liu, C., Yang, S., 2014. CuO nanostructures: synthesis, characterization, growth mechanisms, fundamental properties, and applications. Prog. Mater. Sci. 60, 208–337.